First inactive conformation of CK2α,

the catalytic subunit of protein kinase CK2

Jennifer Raaf[1], Olaf-Georg Issinger[2] and Karsten Niefind[1*]

[1] Universität zu Köln, Institut für Biochemie, Zülpicher Straße 47, D-50674 Köln, Germany

[2]Syddansk Universitet, Institut for Biokemi og Molekylær Biologi, Campusvej 55, DK-5230 Odense, Denmark

**Corresponding author*

E-mail address of the corresponding author:
Karsten.Niefind@uni-koeln.de

Summary

The Ser/Thr kinase CK2 is a heterotetrameric enzyme composed of two catalytic chains (CK2α) attached to a dimer of two non-catalytic subunits (CK2β). CK2α belongs to the superfamily of eukaryotic protein kinases (EPKs). To function as regulatory key components EPKs normally exist in inactive ground states and are activated only upon specific signals. Typically this activation is accompanied by large conformational changes in the helix αC and in the activation segment leading to a characteristic arrangement of catalytic key elements. For CK2α, however, no strict physiological control of activity is known. Accordingly, CK2α was found so far exclusively in the characteristic conformation of active EPKs, which is in this case, additionally stabilized by a unique intramolecular contact between the N-terminal segment on the one side and the helix αC and the activation segment on the other. We report here the structure of a C-terminally truncated variant of human CK2α in which the enzyme adopts for the first time a decidedly inactive conformation. In this CK2α structure those regulatory key regions still are in their active positions. Yet the glycin-rich ATP-binding loop, which is normally part of the canonical anti-parallel β-sheet, has collapsed into the ATP binding site so that ATP is excluded from binding; specifically the side chain of Arg47 occupies the ribose region of the ATP site and Tyr50 the space required by the triphospho moiety. We discuss some factors that may support or disfavour this inactive conformation, among them coordination of small molecules at a remote cavity at the CK2α/CK2β interaction region and binding of a CK2β dimer. The latter stabilizes the glycine-rich loop in the extended active conformation known from the majority of CK2α structures. Thus the novel inactive conformation provides for the first time a structural basis for the stimulatory impact of CK2β on CK2α.

Keywords

Protein kinase CK2; casein kinase 2; CMGC family of the eukaryotic protein kinases; inactive conformation of CK2α; regulation of catalytic activity

Running title:

An inactive conformation of protein kinase CK2α

Abbreviations used:

AMPPNP, adenylyl imidodiphosphate; CDK; cyclin-dependent kinase; CMGC, subgroup of the eukaryotic protein kinases denoted after the **c**yclin-dependent kinases, the **m**itogen-activated protein kinases, **g**lycogen synthase kinase 3 and the **c**ell division control 2-like kinases; CK2, casein kinase 2; CK2α, catalytic subunit of CK2; CK2β, non-catalytic subunit of CK2; *hs*CK2α$^{1\text{-}335}$, C-terminal deletion mutant of human CK2α; *zm*CK2α, CK2α from *Zea maize*; DRB, 5,6-dichlorobenzimidaziole ribofuranoside; EPK, eukaryotic protein kinase; PDB, Protein Data Bank; RMS, root mean square.

Eukaryotic protein kinases (EPKs) catalyze the transfer of the γ-phospho group of ATP to the terminal hydroxy groups of specific serine, threonine and tyrosine residues within substrate proteins. In this way they act as molecular switches orchestrating almost all fundamental cellular processes as components of signalling pathways and regulatory networks[1]. To assure the spatial and temporal interplay of molecular processes, EPKs themselves are in general strictly regulated[2] and dysregulations can lead to cell transformation and cancer.

With regard to their structures EPKs are closely related proteins. They share the same core architecture, consisting of an N-terminal domain based on a central anti-parallel β-sheet and an α-helical C-terminal domain with the active site located in between. Typically EPKs exist in ground states of minimal activity and are activated in response to stimulatory signals[2]. The mechanisms to change from the "off" to the "on" state include binding of activator proteins [(cyclin-dependent kinases (CDKs)], release of regulatory subunits [cAMP-dependent protein kinase], phosphorylation [mitogen-activated protein kinases], dephosphorylation [glycogen-synthase kinase 3], release of pseudosubstrate segments (twitchin kinase), dimerization (RNA-activated protein kinase, EGF receptor) or combinations of these[2,3,4]. In general these regulatory events are accompanied with large conformational changes, in particular in the two regulatory key elements, the so-called activation segment at the border of the C-terminal domain and the helix αC in the N-terminal domain[2].

EPKs are conformationally individual and diverse in their inactive states, but they adopt a similar conformation in the "on" state due to the chemical constraints of the phospho transfer reaction[2]. In this conformation the activation segment is open to allow substrate binding[5] whereas it is often non-productively rearranged in the "off" state. Moreover, in active EPKs the helix αC is orientated such that a conserved glutamate residue can establish a salt bridge to a likewise conserved lysine residue; fixed in this way the lysine side chain can coordinate the α- and β-phospho groups of ATP in their functional conformations. This lysine/glutamate ion pair is often absent in inactive EPKs and is therefore regarded as a sensitive identification for the active conformation of an EPK[2].

The importance of activity control for EPK function makes the exploration of regulatory mechanisms and their structural bases a fundamental subject of EPK research. In this respect the regulation of protein kinase CK2 (former name: casein kinase 2) – a heterotetrameric Ser/Thr kinase composed of two separate catalytic chains (CK2α) attached to a central dimer of two non-catalytic subunits (CK2β)[6] - is particularly puzzling since none of the above-mentioned control mechanisms works in this case. Thus, although CK2 itself is a regulatory factor in apotosis, proliferation[7,8]and multiple transitions in the cell cycle[9], its own regulation is poorly understood[10]. CK2α alone has a significant basal catalytic activity, which is enhanced by CK2β as long as peptides serve as substrates[11]. With complete proteins as substrates, however, the modulatory impact of CK2β on CK2α is more diverse and can sometimes involve even down-regulation, e.g. in the case of calmodulin[12]. At any rate, CK2β is no on/off switch for CK2α and thus not comparable to the cyclins in the case of the CDKs.

Various alternative notions of CK2 regulation have been considered so far, e.g.: (i) formation of inactive filamentous aggregates from heterotetrameric CK2 holoenzyme complexes[13]; (ii) regulation through small molecules like inositol phosphates[14]; (iii) modulation of specificity through protein-protein interactions[15,16]; (iv) intracellular translocation[17]; (v) long-term regulation via the enzyme concentration through gene expression and protein degradation[18].

None of these regulatory concepts requires an underlying inactive CK2α conformation. Thus, they are consistent with the fact that in more than 30 crystal structures CK2α was found exclusively in the typical conformation of active EPKs and that this active conformation is in the case of CK2α particularly constrained by at least three internal elements: (i) the N-terminal segment that fixes the activation segment and the helix αC in a way comparable to the cyclins in the case of the CDKs[19]; (ii) an exceptional tryptophane in the magnesium binding loop[5] which replaces the central Phe residue of the canonical DFG motif: this Trp side chain allows an additional hydrogen bond[19] that disfavours "DFG-out" conformations as known from inactive mitogen-activated protein kinases[20]; (iii) a

structural chloride ion together with a conserved water cluster that supports the contact between N-terminal segment and activation segment[21].

In accordance with these and further structural features it was proposed that CK2α was "evolved to be active"[22] and can possibly never occur in an inactive conformation. Therefore, we were surprised to discover a decidedly inactive conformation of human CK2α. Here, we describe this structure. We propose on its basis a concept for the stimulatory impact of CK2β on CK2α and moreover discuss its possible consequences for CK2 regulation.

Co-crystallization of a *hs*CK2α$^{1-335}$ and glycerol

The inactive CK2α conformation was found by coincidence when we co-crystallized glycerol with *hs*CK2α$^{1-335}$, a C-terminal deletion mutant of human CK2α that is catalytically fully active[23] and capable to associate with CK2β[24]. The motivation for this co-crystallization was based on a recent report that the CK2α/CK2β interface region of human CK2α harbours a relatively unspecific small-molecule binding site[25] to which we refer from here on as the "remote cavity" in order to distinguish it from the canonical ATP-binding site.

In that study[24] the remote cavity was occupied by 5,6-dichlorobenzimidaziole ribofuranoside (DRB) in a complex structure with *hs*CK2α$^{1-335}$ and by glycerol in complex with the mutant *hs*CK2α$^{1-335}$-V66A/M163L. In this context it became evident that the occupation of the remote cavity has a subtle impact on the crystallization behaviour of the enzyme enforcing a certain tetragonal crystal packing and salts like ammonium sulfate or sodium citrate as precipitating agents (rather than polyethylene glycols as in all previous crystallization reports with CK2α[26]). Such an impact should be mediated by either novel possibilities for crystalline contacts through the small molecule or by an influence on the enzyme's 3D structure or by a combination of both.

This notion should be substantiated by the co-crystallization of glycerol and *hs*CK2α$^{1-335}$. As expected the *hs*CK2α$^{1-335}$/glycerol crystals appeared under high concentrations of ammonium sulfate

and possess the same apparent space group ($P4_32_12$) and lattice constants (Tab. 1) as observed in the previously described cases[25]. As shown below the remote cavity in the *hs*CK2α$^{1-335}$/glycerol complex is in fact occupied by a glycerol molecule (Fig. 1a/b), meaning a certain correlation between the occupation of the remote cavity and the crystallization properties of *hs*CK2α$^{1-335}$ seems to exists.

Structure of a human CK2α$^{1-335}$/glycerol complex

The *hs*CK2α$^{1-335}$/glycerol crystals diffracted to 2.3 Å resolution, and the corresponding structure was refined to acceptable R-values and stereochemical characteristics (Tab. 1). In the course of the refinement the apparent crystal symmetry had to be reduced to space group $P4_3$ combined with perfect merohedral twinning. While with the higher symmetry some important parts of the structure remained disordered, the consideration of twinning resulted in interpretable electron density in these regions.

The asymmetric unit of the crystals is occupied by two *hs*CK2α$^{1-335}$ chains arranged as a dimer with C_2 point symmetry (Fig. 1a). We submitted the *hs*CK2α$^{1-335}$ dimer to the PISA server[27] which reported a value of 1295.7 Å^2 for the interface between the two monomers. This value is within the range typically found for homodimers with a monomeric molecular mass around 40 kDa[28]. Interestingly, the final seven residues of the *hs*CK2α$^{1-335}$ construct are involved in the homodimeric interaction; this observation suggests that the 57 residues longer C-terminal segment of wildtype human CK2α might further support the dimerization. On the other hand the PISA server[27] – taking into account more criteria than just the interface size - does not predict a stable quaternary structure for *hs*CK2α$^{1-335}$ in solution which is consistent with data from ultracentrifugation studies with human CK2α[29]. Thus, it is open whether the dimeric arrangement shown in Fig. 1a has any relevance apart from the crystalline state.

A structural comparison of the two *hs*CK2α$^{1-335}$ protomers revealed some minor differences between them but the main feature we describe below – the blockade of the ATP-binding site – is visible in both cases; therefore, we restrict the following discussion to subunit A in which the remote

cavity is occupied by a glycerol molecule (Fig. 1a/b). This glycerol molecule overlaps partly with the remote cavity ligands of the *hs*CK2α$^{1-335}$/DRB complex and of the *hs*CK2α$^{1-335}$-V66A/M163L/glycerol complex, but it sticks less deep in the cavity and leaves space for an additional water molecule (Fig. 1b). Apart from the remote cavity ligand each of the *hs*CK2α$^{1-335}$ chains harbours a further glycerol molecule at the C-terminal domain (Fig. 1a).

We fitted the novel *hs*CK2α$^{1-335}$ structure globally on the *hs*CK2α$^{1-335}$/DRB complex[25] (Fig. 2a). Both structures are embedded in a similar crystalline environment so that any conformational deviations are most probably not caused by crystal packing constraints. While by far the largest structural differences occur in the glycin-rich ATP-binding loop (Fig. 2a), both structures are similar in the hinge region that connects the two main domains of the enzyme and functions as an anchor for the adenine group of ATP. A recent comparative analysis has revealed that two principle conformations – an open and a closed one – exist for the hinge region of human CK2α[30]. Hence, the *hs*CK2α$^{1-335}$/glycerol structure belongs to the same cluster as the *hs*CK2α$^{1-335}$/DRB complex, namely the closed one.

Moreover, the major elements of EPK regulation – the activation segment and the helix αC – are essentially identical in the two structures compared in Fig. 2a, meaning in the novel *hs*CK2α$^{1-335}$/glycerol structure they adopt the typical arrangement of active EPKs[2]. Nevertheless, we characterize this structure as "inactive" for two reasons: first the above-mentioned Lys/Glu ion pair (Lys68 and Glu81 in the case of CK2α) which is required for productive ATP binding is no longer present, rather the side chain of Lys68 is coordinated by the negative charges of Asp175 (the magnesium binding aspartate in the productive state[31]) and a nearby chloride ion (Fig. 3c); second the ATP binding site is completely blocked as a result of a collapse of the glycin-rich loop (Fig. 3a).

A collapse of the glycin-rich loop blocks the ATP-binding site

The glycin-rich loop comprises the first two strands (β1 and β2) of the anti-parallel β-sheet within the

N-terminal domain plus the interconnecting reverse turn (Fig. 2b). The prototype of the loop for active CK2α occurred in a complex of maize CK2α with AMPNP (blue tube in Fig. 2b) in which both the loop and the complete nucleotide were found as well defined by electron density[31,32]. Here, the loop is as extended as possible, meaning strand β1 ranges with good β-strand geometry up to Gly48, strand β2 starts with Ser51 and the reverse turn comprises only the two tip residue, i.e. Lys49 and Tyr50. Two glycine residues (Gly46 and Gly48) confer the loop a certain flexibility which is balanced, however, by the integration of the two strands into the bigger β-sheet (Fig. 2b).

The extended glycin-rich loop is found essentially in all CK2α structures (see representative examples in Fig. 2b), even including the complex of maize CK2α with the ATP-competitive inhibitor emodin (black tube in Fig. 2b), for which the biggest deviation of the glycin-rich loop from the canonical conformation has been reported so far[33]. In the CK2 holoenzyme[6] the active conformation of the glycine-rich loop is additionally stabilized by the CK2β dimer (yellow and magenta chain in Fig. 2b) which is in contact with all five strands of the β-sheet.

Against this background, the collapse of the glycine-rich loop in the *hs*CK2α$^{1-335}$/glycerol structure is particularly striking. It is correlated with a reduction of the strands β1 and β2 by two residues each (Fig. 2b). The collapse results in a blockade of the ATP-binding site as clearly indicated by the fact that it is not occupied by the ATP-analogue AMPPNP, although such a substance was present in significant concentration in the crystallization drop.

A comparison with the complex structure of *hs*CK2α$^{1-335}$ and AMPPNP (PDB code 2PVR)[22] reveals the detailled structural basis of this fact: Tyr50, Arg47 and the surrounding loop region are folded in a way that prevents nucleotide binding (Fig. 3a). Arg47 is directed into a part of the canonical ATP binding site that was referred to as “sugar region”[34]; after a large movement of the Arg47 side chain its terminal guanidinium group forms a close hydrogen bond to His160, which itself is turned towards the critical region, and a salt bridge with Asp120 from the hinge region (Fig. 3a).

A second remarkable residue of the glycine-rich loop is Tyr50. In the active conformation of *hs*CK2α$^{1\text{-}335}$ [22] its side chain is coordinated by Lys74 and Lys77 (Fig. 3b) while in the inactive form it bends down to the absolutely conserved catalytic aspartate (Asp156) and obtains the space normally required for the triphospho moiety of ATP (Fig. 3b). Thus, in a way an early notion of Allende & Allende[10] that Tyr50 of CK2α – like its equivalent Tyr15 of CDK2[35] - may serve to downregulate the enzyme receives a certain confirmation – albeit the mechanism is not phosphorylation as in the case of CDK2 but conformational change.

Which factors support or disfavour the inactive CK2α conformation?

The structure we describe here expands the knowledge about the conformational possibilities of CK2α. In spite of the structural conservation of the EPK-typical control elements (helix αC and activation segment) the enzyme can exist either in an active or in an inactive conformation concerning the glycine-rich loop – or in an equilibrium of both.

Unlike other EPKs phosphorylation has no impact on the transition between both activation states. Rather the inherent plasticity of the glycin-rich loop may support the interchange between them. Additionally, there may be external factors favouring either of the two states and thus affecting the putative conformational equilibrium, for instance:

(i) Crystal packing

The trivial case would be that the inactive CK2α conformation is a result of crystallization or crystal dehydration. Such artefacts can never be excluded in protein crystallography; however, we can at least state that crystal packing is not a sufficient condition to cause the glycin-rich loop to collapse since in the two aforementioned references cases, which are examples with similar crystallization conditions and crystal parameters[24], the active conformation was found, and the ATP-binding site was occupied with DRB in one case and with AMPPNP in the other.

(ii) Small-molecule binding to the remote cavity

Does glycerol binding to the remote cavity promote the glycin-rich loop collapse? To check this possibility we performed a series of catalytic activity tests with *hs*CK2α$^{1-335}$ and increasing concentrations of glycerol, but we could not detect any inhibition by glycerol.

In the case of DRB, however, the occupation of the remote cavity correlated with a non-ATP-competitive inhibition effect[24]. Recently Laudet et al.[36] reported that certain CK2β-antagonists both can interfere with the CK2α/CK2β interaction and inhibit isolated CK2α; this inhibition can be overcome by increasing concentrations of CK2β, but not of ATP. Obviously, CK2α coordinates these substances in the CK2α/CK2β interface region, rather than at the ATP-binding site, but is nevertheless down-regulated by them. So far it is unknown which conformational changes in CK2α are induced by these substances but the inactive conformation we describe here provides a plausible model.

(iii) CK2β

While certain small molecules may enforce the inactive conformation of the glycine-rich loop, CK2β probably acts in the opposite direction. In the CK2 holoenzyme[6] the CK2β dimer binds to the other surface to the N-terminal β-sheet which is thereby stabilized (Fig. 2b) preventing a collapse of the glycine-rich loop.

This mechanistic model is consistent with the basal activation of CK2α by CK2β[29]. As in the case of calmodulin phosphorylation[12] this stimulatory impact can be covered by remote interactions, but it becomes apparent when small peptides – like the significant phospho acceptor peptide from calmodulin[29] - are used as substrates.

Conclusion

We desribe here for the first time an inactive structure of human CK2α in which the ATP-binding site is blocked by the glycine-rich loop that normally serves for ATP coordination. This structure together with further observations, we mentioned above, leads to a working hypothesis summarized

in Fig. 4: CK2α predominantly adopts an active conformation which is nevertheless in a reversible equilibrium with an inactive state. Certain small molecules – artifical ones, but possibly also physiological metabolites - can bind to the remote cavity and shift the equilibrium towards the inactive form, whereas CK2β displaces such ligands from the CK2α/CK2β interface region and stabilizes simultaneously the extended and active form of the glycin-rich loop. In this way CK2β removes active CK2α from the equilibrium which is thus completely transferred to the active side.

This working hypothesis integrates the current structural and enzymological knowledge about CK2α. Nevertheless, it has to be substantiated by further experimental work. It will be particularly interesting in the future whether metabolites or synthetic small molecules can be found with the potential to shift CK2α to the inactive conformation.

Acknowledgments.

We are grateful to Elena Brunstein for technical assistence. This work was funded by the Danish Research Council (grant no. 21-01-0511) and by the Deutsche Forschungsgemeinschaft (DFG; grant NI 643/1-3).

Accession codes.

The atomic coordinates and structure factor amplitudes of the inactive *hs*CK2α$^{1-335}$/glycerol structure are available from the PDB under the accession code 3FWQ.

References

[1] Manning, G., Plowman, G. D., Hunter, T. & Sudarsanam S. (2002). Evolution of protein kinase signaling from yeast to man. *Trends Biochem. Sci.* **27**, 514-520.

[2] Huse, M. & Kuriyan, J. (2002). The conformational pasticity of protein kinases. *Cell* **109**, 275-282.

[3] Pellicena, P. & Kuriyan, J. (2006). Protein-protein interactions in the allosteric regulation of protein kinases. *Curr. Opin. Struct. Biol.* **16**, 702-709.

[4] Johnson, L.N., Noble, M.E. & Owen, D.J. (1996). Active and inactive protein kinases: structural basis for regulation. *Cell*. **85**. 149-58.

[5] Nolen, B., Taylor, S. & Ghosh, G. (2004). Regulation of protein kinases: controlling activity through activation segment conformation. *Mol. Cell* **15**, 661-667.

[6] Niefind, K., Guerra, B., Ermakowa, I. & Issinger, O.-G. (2001). Crystal structure of human protein kinase CK2: insights into basic properties of the CK2 holoenzyme. *EMBO J*. **20,** 5320–5331.

[7] Guerra, B. & Issinger, O.-G (1999). Protein kinase CK2 and its role in cellular proliferation, development and pathology. *Electrophoresis*. **20**. 391-408.

[8] Guerra, B. & Issinger, O.-G. (2008). Protein kinase CK2 in human diseases. *Curr. Med. Chem.* **15**, 1870-1886.

[9] Litchfield, D. W. (2003). Protein kinase CK2: structure, regulation and role in cellular decisions of life and death. *Biochem. J*. **369**. 1–15.

[10] Allende, J. E. & Allende, C. C. (1995). Protein kinase CK2: an enzyme with multiple substrates and a puzzling regulation. *FASEB J.* **9**, 313-323.

[11] Grankowski, N., Boldyreff, B. & Issinger, O.-G. (1991). Isolation and characterization of recombinant human casein kinase II subunits α and β from bacteria. *Eur. J. Biochem.* **198**, 25-30.

[12] Bidwai, A. P., Reed, J. C. & Glover, C. V. C. (1993). Phosphorylation of calmodulin by the catalytic subunit of casein kinase II is inhibited by the regulatory subunit. *Arch. Biochem.*

Biophys. **300**, 265-270.

[13] Niefind, K. & Issinger, O.-G. (2005). Primary and secondary interactions between CK2α and CK2β lead to ring-like structures in the crystals of the CK2 holoenzyme. *Mol. Cell. Biochem.* **274,** 3-14.

[14] Solyakov, L., Cain, K., Tracey, B. M., Jukes, R., Riley, A. M., Potter, B. V. & Tobin, A. B. (2004). Regulation of casein kinase-2 (CK2) activity by inositol phosphates. *J. Biol. Chem.* **279**, 43403-43410.

[15] Keller, D.M. & Lu, H. (2002). p53 serine 392 phosphorylation increases after UV through induction of the assembly of the CK2·hSPT16·SSRP1 complex. *J. Biol. Chem.* **277**, 50206-50213.

[16] Filhol, O., Martiel, J. L. & Cochet, C. (2004). Protein kinase CK2: a new view of an old molecular complex. *EMBO J.* **5**, 351-355.

[17] Bosc, D. G., Graham, G. C., Saulnier, R. B., Zhang, C. ,Prober, D., Gietz R. D. & Litchfield, D. W. (2000). Identification and characterization of CKIP-1, a novel pleckstrin homology domain-containing protein that interacts with protein kinase CK2. *J. Biol. Chem.* **275**, 14295-14306.

[18] Zhang, C., Vilk, G., Canton, D. A. & Litchfield, D. W. (2002). Phosphorylation regulates the stability of the regulatory CK2 subunit. *Oncogene* **21**, 3754-3764.

[19] Niefind, K., Guerra, B., Pinna, L. A., Issinger, O.-G. & Schomburg, D. (1998). Crystal structure of the catalytic subunit of protein kinase CK2 from *Zea mays* at 2.1 Å resolution. *EMBO J.* **17,** 2451-2462.

[20] Pargellis, C., Tong, L., Churchill, L., Cirillo, P. F., Gilmore, T., Graham, A. G., Grob, P. M., Hickey, E. R., Moss, N., Pav, S. & Regan, J. (2002). Inhibition of p38 MAP kinase by utilizing a novel allosteric binding site. *Nat. Struct. Biol.* **9**, 268-272.

[21] Raaf, J., Issinger, O.-G. & Niefind, K. (2008). Insights from soft X-rays: the chlorine and sulfur sub-structures of a CK2α/DRB complex. *Mol. Cell. Biochem*. **316**, 15-23.

[22] Niefind, K., Yde, C. W., Ermakova, I. & Issinger, O.-G. (2007). Evolved to be active: sulfate ions define substrate recognition sites of CK2α and emphasise its exceptional role within the CMGC family of eukaryotic protein kinases. *J. Mol. Biol*. **370**, 427-438.

[23] Ermakova, I., Boldyreff, B., Issinger, O.-G. & Niefind, K. (2003). Crystal structure of a C-terminal deletion mutant of human protein kinase CK2 catalytic subunit. *J. Mol. Biol*. **330**,925-934.

[24] Raaf, J., Brunstein, E., Issinger, O.-G. & Niefind, K. (2008). The interaction of CK2α and CK2β, the subunits of protein kinase CK2, requires CK2β in a pre-formed conformation and is enthalpically driven. *Protein Sci.*, in press

[25] Raaf, J., Brunstein, E., Issinger, O.-G. & Niefind, K. (2008). The CK2α/CK2β interface of human protein kinase CK2 harbors a binding pocket for small molecules. *Chem. Biol.* **15**, 111-117.

[26] Guerra, B., Niefind, K., Pinna, L. A., Schomburg, D. & Issinger, O.-G. 1998). Expression, purification and crystallization of the catalytic subunit of protein kinase CK2 from *Zea mays*. *Acta Crystallogr.* **D54**, 143-145.

[27] Krissinel, E. & Henrick, K. (2007). Inference of macromolecular assemblies from crystalline state. *J. Mol. Biol.* **372**, 774-797.

[28] Jones, S. & Thornton, J.M. (1996). Principles of protein-protein interactions. *Proc. Natl. Acad. Sci. U. S. A.* **93**, 13-20.

[29] Boldyreff, B., Meggio, F., Pinna, L. A. & Issinger, O.-G. (1993). Reconstitution of normal and hyperactivated forms of casein kinase-2 by variably mutated β-subunits. *Biochemistry* **32**, 12672-12677.

[30] Raaf, J., Klopffleisch, K., Issinger, O.-G. & Niefind, K. (2008). The catalytic subunit of human protein kinase CK2 structurally deviates from ist maize homologue in complex with the nucleotide competitive inhibitor emodin. *J. Mol. Biol.* **377**, 1-8.

[31] Niefind, K., Pütter, M., Guerra, B., Issinger, O.-G. & Schomburg, D. (1999). GTP plus water mimic ATP in the active site of protein kinase CK2. *Nat. Struct. Biol.* **6**, 1100-1103.

[32] Yde, C. W., Ermakova, I., Issinger, O.-G. & Niefind, K. (2005). Inclining the purine base binding plane in protein kinase CK2 by exchanging the flanking side-chains generates a preference for ATP as a cosubstrate. *J. Mol. Biol.* **347**, 399-414.

[33] Battistutta, R., Sarno, S., De Moliner, E., Papinutto, E., Zanotti, G. & Pinna, L. A. (2000). The replacement of ATP by the competitive inhibitor emodin induces conformational modifications in the catalytic site of protein kinase CK2. *J. Biol. Chem.* **275**, 29618-29622.

[34] Traxler, P. & Furet, P. (1999). Strategies toward the design of novel and selective protein tyrosine kinase inhibitors. *Pharmacol. Ther.* **82**, 195-206.

[35] Welburn, J. P., Tucker, J. A., Johnson, T., Lindert, L., Morgan, M., Willis, A., Noble, M. E. & Endicott, J. A. (2007). How tyrosine 15 phosphorylation inhibits the activity of cyclin-dependent kinase 2-cyclin A. *J. Biol. Chem.* **282**, 3173-3181.

[36] Laudet, B., Moucadel, V., Prudent, R., Filhol, O., Wong, Y.-S., Royer, D. & Cochet, C. (2008). Identification of chemical inhibitors of protein kinase CK2 subunit interaction. *Mol. Cell. Biochem.* **316**, 63-69.

[37] DeLano, W. L. "The PyMOL Molecular Graphics System." DeLano Scientific LLC, San Carlos, CA, USA.

[38] Esnouf, R. M. (1997). An extensively modified version of MolScript that includes greatly enhanced coloring capabilities. *J. Mol. Graph.* **15**, 132-134.

[39] Merritt, E.A., and Bacon, D.J. (1997). Raster3D: photorealistic molecular graphics. *Methods Enzymol.* **277**, 505-524.

[40] Collaborative Computational Project, Number 4 (1994). The CCP4 suite: programs for protein crystallography. *Acta Crystallogr.* **D50**, 760-763.

[41] Schomburg, D. & Reichelt, J. (1988). BRAGI: a comprehensive protein modeling program

system. *J. Mol. Graph.* **6**, 161 - 165.

[42] Otwinowski, Z. & Minor, W. (1997). Processing of X-ray diffraction data collected in oscillation mode. *Methods Enzymol.* **276,** 307-326.

[43] Collaborative Computational Project, Number 4 (1994). The CCP4 suite: programs for protein crystallography. *Acta Crystallogr.* **D50**, 760-763.

[44] Emsley, P. & Cowtan, K. (2004). Coot: model-building tools for molecular graphics. *Acta Crystallogr.* **D60**, 2126-2132.

Figures

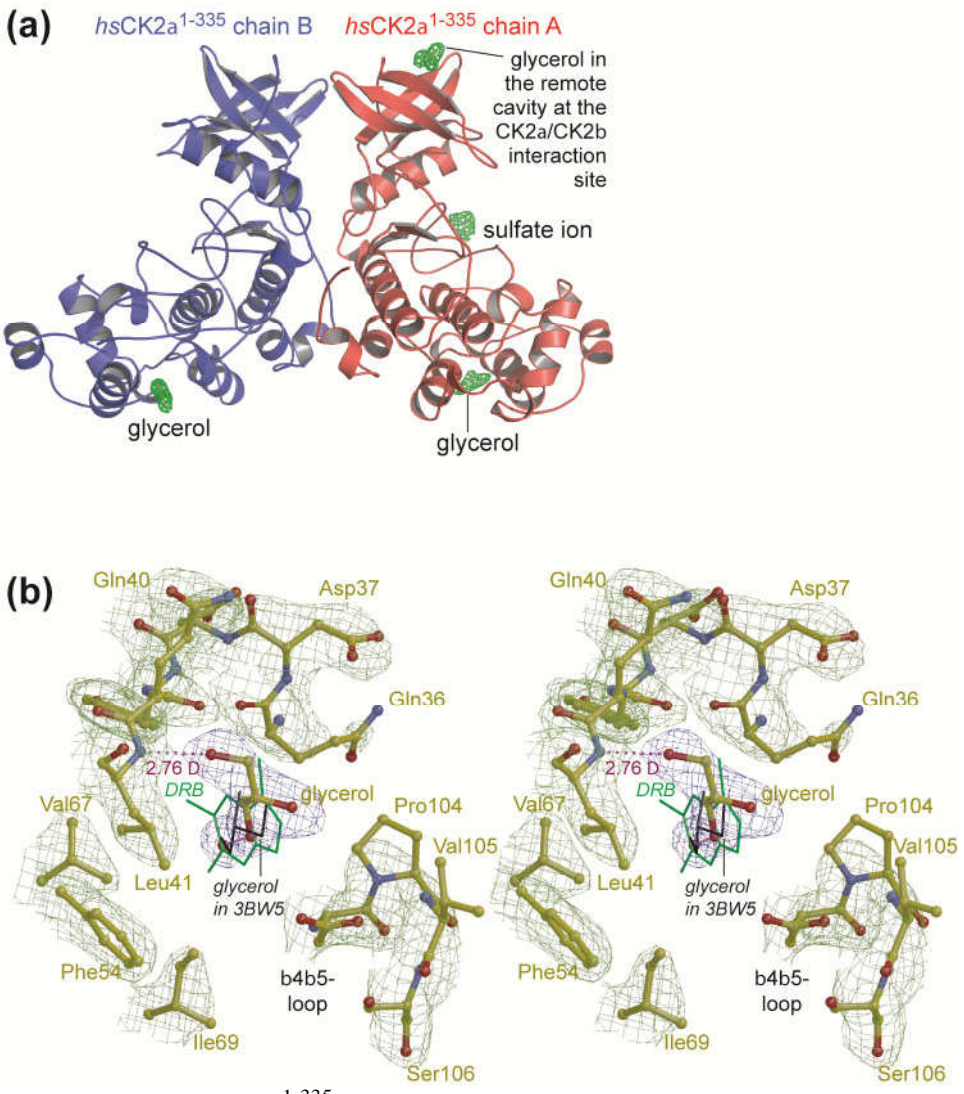

Fig. 1: Glycerol binding at *hs*CK2α$^{1-335}$.

(a) The *hs*CK2α$^{1-335}$ dimer in the crystallographic asymmetric unit. The two *hs*CK2α$^{1-335}$ chains A (red) and B (blue) differ in conformational details and ligands. The pieces of electron density around the ligands were contoured at 1 σ. The figure was drawn with PyMol[37].

(b) Stereo picture of the remote cavity of *hs*CK2α$^{1-335}$ chain A, filled with a glycerol and a water molecule. These two ligands are covered with blue electron density while the surrounding enzyme matrix is embedded in green electron density. The pieces of density were extracted from the final 2Fo-Fc-density; the contouring level was 1 σ. For comparison the glycerol molecule in the *hs*CK2α$^{1-335}$-V66A/M163L structure (PDB code 3BW5[25]) was drawn in black colour and the 5,6-dichloro benzimidazole moiety of the *hs*CK2α$^{1-335}$/DRB complex (PDB code 2RKP[25]) in green colour. Some hydrogen bonds are indicated with dotted lines in magenta colour. The figure was prepared with BOBSCRIPT[38] and Raster3D[39].

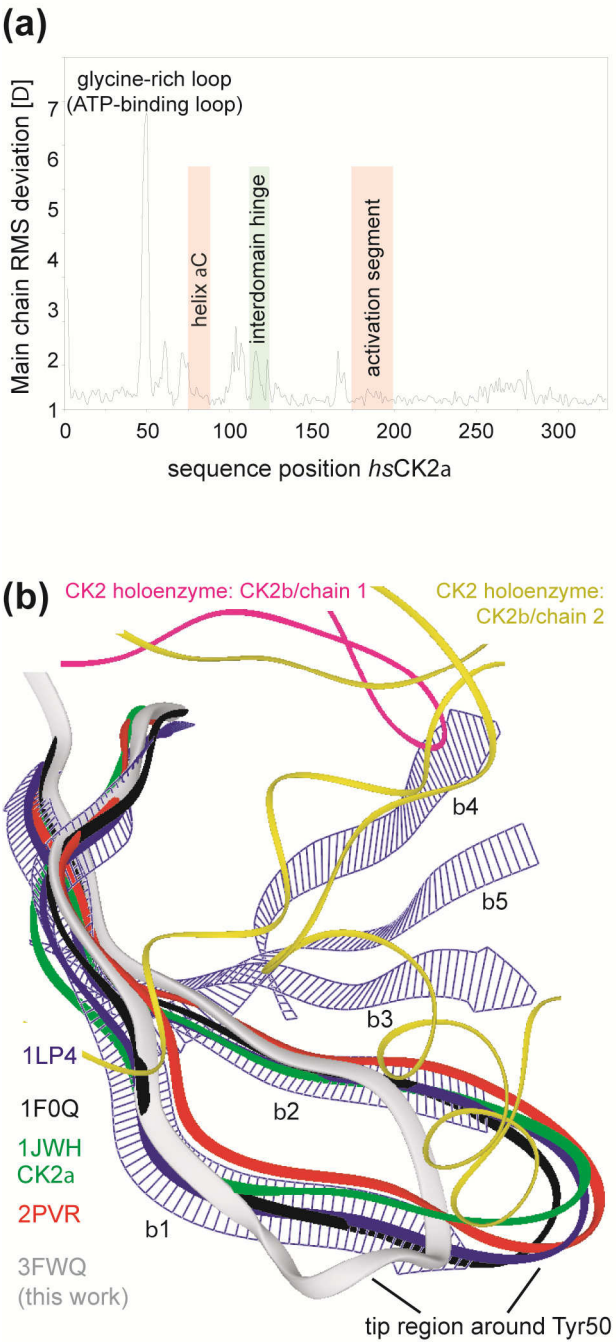

Fig. 2: Structural comparisons.

(a) Global comparison of the *hs*CK2α[1-335]/glycerol structure (this work) with the *hs*CK2α[1-335]/DRB structure[25]. The RMS deviation values averaged over main chain atoms were calculated with the program LSQKAP from the CCP4 suite[40].

(b) The glycine-rich ATP-binding loop as part of the anti-parallel β-sheet in the centre of the N-terminal domain. The fully extended conformation of the loop is found in the *zm*CK2α/AMPPNP complex (1LP4, blue)[31,32], in the *hs*CK2α[1-335]/AMPPNP complex (2PVR, red)[22] and in the human CK2 holoenzyme (1JWH, green)[6]. In the *zm*CK2α/emodin complex (1FOQ, black)[33] certain deviations were found which were, however, not big enough to prevent the coordination of the emodin ligand at the ATP-binding site. The inactive conformation of the glycine-rich loop (this work) is shown in grey colour. The two chains of the CK2β dimer as found in the CK2 holoenzyme[6] were drawn in magenta and yellow colour after structural overlay of the corresponding CK2α chains. The figure was prepared with BRAGI[41].

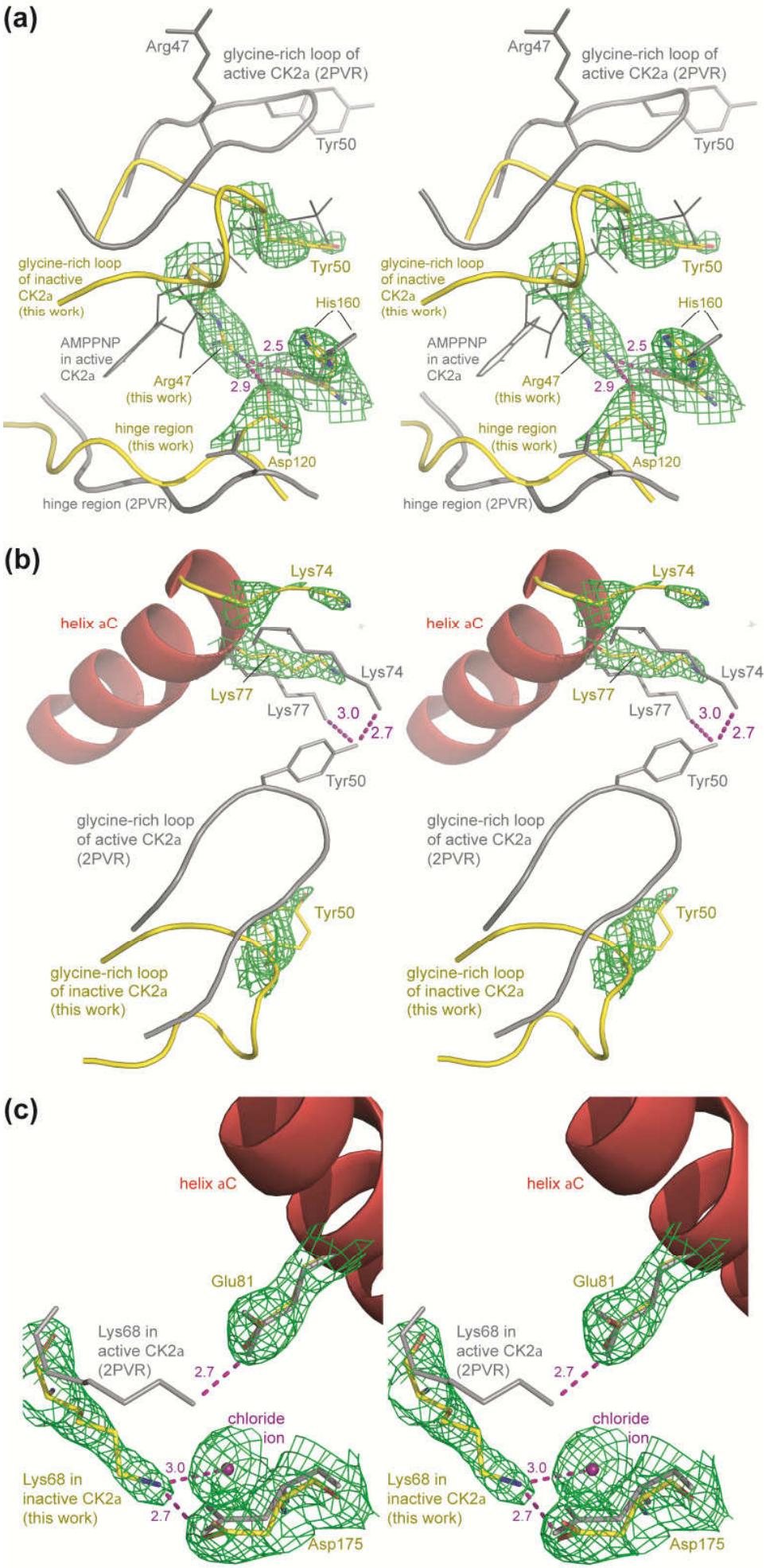
(a)
Arg47
glycine-rich loop of active CK2a (2PVR)
Tyr50
glycine-rich loop of inactive CK2a (this work)
Tyr50
His160
AMPPNP in active CK2a
2.5
Arg47 (this work)
2.9
hinge region (this work)
Asp120
hinge region (2PVR)
Arg47
glycine-rich loop of active CK2a (2PVR)
Tyr50
glycine-rich loop of inactive CK2a (this work)
Tyr50
His160
AMPPNP in active CK2a
2.5
Arg47 (this work)
2.9
hinge region (this work)
Asp120
hinge region (2PVR)
(b)
Lys74
helix aC
Lys74
Lys77
Lys77
3.0
2.7
Tyr50
glycine-rich loop of active CK2a (2PVR)
Tyr50
glycine-rich loop of inactive CK2a (this work)
Lys74
helix aC
Lys74
Lys77
Lys77
3.0
2.7
Tyr50
glycine-rich loop of active CK2a (2PVR)
Tyr50
glycine-rich loop of inactive CK2a (this work)
(c)
helix aC
Glu81
Lys68 in active CK2a (2PVR)
2.7
chloride ion
3.0
Lys68 in inactive CK2a (this work)
2.7
Asp175
helix aC
Glu81
Lys68 in active CK2a (2PVR)
2.7
chloride ion
3.0
Lys68 in inactive CK2a (this work)
2.7
Asp175

Fig. 3: Details of the inactive CK2α conformation.

Three stereo pictures were prepared with PyMol[37] after structural superimposition of active CK2α in complex with AMPPNP (2PVR[22]) and inactive CK2α (this work). The grey colour for structural elements and labels refers to active CK2α. All pieces of electron density were extracted from the final 2Fo-Fc map using a contouring level 0.9 σ. Some hydrogen bonds are indicated with dotted lines in magenta colour and donor/acceptor distances given in Å.

(a) The core of the ATP-binding site is occupied by AMPPNP in active CK2α, but with Arg47 and Tyr50 in the active case after the collapse of the glycine-rich loop.

(b) The anchoring of the tip of the glycine-rich loop conformation in active CK2α by two lysine side chains from the helix αC is broken in inactive CK2α. This allows the tip residue Tyr50 to move into the region normally occupied by the triphospho moiety of the ATP.

(c) Disruption of the conserved Lys68/Glu81 ion pair found in active CK2α. This salt bridge is a characteristic feature of active EPKs[2] because it is a necessary condition for the correct coordination of the α- and β-phospho group of ATP.

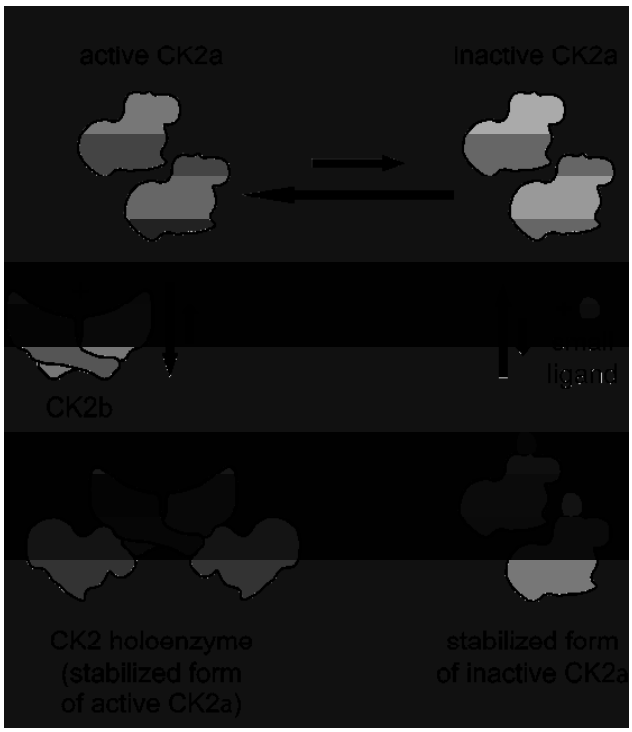

Fig. 4: Working hypothesis to illustrate the potential regulation of CK2α by CK2β and by small molecules.

Tables

Table 1: X-ray diffraction data collection and refinement statistics.

Diffraction data collection	
Temperature [K]	100
Space group	$P4_3$
Cell dimensions	
a, b, c [Å]	71.32, 71.32, 125.68
α, β, γ [°]	90.0, 90.0, 90.0
Resolution [Å]	34.50-2.30 (2.38-2.30)[1]
R_{sym} [2]	10.0 (72.4)[1]
Signal to noise ratio (I/σ_I)	17.6 (2.0)[1]
No. of unique reflections	26999
Completeness [%]	96.9 (98.3)[1]
Redundancy	7.7 (7.2)[1]
B-factor from Wilson plot [$Å^2$]	47.1
Refinement	
Resolution [Å]	34.5 - 2.3
No. of refl. in working set/test set	25746/1253
R_{work} / R_{free}	17.0/23.3
No. of atoms	
Protein	5634
Ligand/ion	28
Water	204
B-factors	
Protein	41.4
Ligand/ion	46.3
Water	33.2
R.m.s deviations	
Bond lengths [Å]	0.006
Bond angles [°]	0.885

[1] values in parentheses are for highest resolution shell

[2] $R_{sym} = \Sigma_h\Sigma_j|I_{h,j} - \langle I_{ch}\rangle| / \Sigma_h\Sigma_j I_{h,j}$, where $I_{h,j}$ is the intensity of the jth observation of unique reflection h, and $\langle I_h\rangle$ is the mean intensity of that reflection. Friedel mates were merged.

*Hs*CK2α$^{1-335}$ was prepared as described[22]. The purified proteins were concentrated and rebuffered in 500 mM NaCl, 25 mM Tris/HCl, pH 8.5, by ultrafiltration using AMICON Ultra-15 tubes. The crystallization experiments were performed at 20 °C with the sitting-drop variant of the vapor diffusion technique using the "Jena Bioscience-Screen 6" from Jena Bioscience. The crystallization drops were prepared as master mixes and each drop contained 1 µl of *hs*CK2α$^{1-335}$ (10mg/ml), 3 µl 1-mM AMPPNP, 0.6 µl 10-mM $MgCl_2$, 0.1 µl glycerol (100%) and 1 µl reservoir solution composed of 2-M ammonium sulfate and 2-M NaCl. Cryo conditions were obtained by reequllibration after changing the reservoir to 3.9-M ammonium sulfate.

X-ray diffraction data were collected at the beamline X12 of the EMBL outstation in Hamburg. The wavelength of the X-rays was 0.9537 Å. The data collection temperature was 100 K. All diffraction data were processed with the HKL package[42]. The *hs*CK2α$^{1-335}$/glycerol structure was determined by molecular replacement using MOLREP from the CCP4 suite[43] and the structure of *hs*CK2α$^{1-335}$ (PDB file 2PVR[22]) as a search model. For the refinement we used REFMAC[43]. Manual corrections were performed with COOT[44].